

10  
10-24-90 JS①

CONF-9009276-1

SLAC-PUB-5329  
August 1990  
(A)

# A SUMMARY OF GROUND MOTION EFFECTS AT SLAC RESULTING FROM THE OCT 17TH 1989 EARTHQUAKE\*

R.E.Ruland

SLAC-PUB--5329

*Stanford Linear Accelerator Center, Stanford  
University, Stanford, CA 94309 USA*

DE91 001030

## 1. ABSTRACT

Ground motions resulting from the October 17th 1989 (Loma Prieta) earthquake are described and can be correlated with some geologic features of the SLAC site. Recent deformations of the linac are also related to slow motions observed over the past 20 years. Measured characteristics of the earthquake are listed. Some effects on machine components and detectors are noted.

## 2. INTRODUCTION

The original builders of the Stanford Linear Accelerator Center payed a great deal of attention to questions of site suitability. At that time, (early 1960's) before steering and focussing was introduced along the linac, it was then believed that the accelerator should remain aligned along a straight line ranging from within .03 inches in 250 feet to 1 inch in 10,000 feet for periods up to one year and 5 inches for "as long as possible".<sup>[1]</sup> The proximity of the San Andreas fault system has been commented on at length, but every responsible geologist then, as now, has stated that although earthquakes, and more interestingly their effects, can not be predicted with accuracy, "it is most unlikely that the accelerator tunnel will be damaged unless it crosses a fault which ruptures or is located within a zone of 'maximum intensity' or in terrain with potentially unstable topography and/or incompetent rock." We shall see that this belief has been borne out at SLAC up to, and including, the recent past.

\* Work supported by the Department of Energy, contract DE-AC03-76SF00515.

eb

MASTER

*Presented at the 2nd International Workshop on Accelerator Alignment,  
Hamburg, Germany, September 10-12, 1990*

### 3. PROPERTIES OF THE OCTOBER 17th 1989 EARTHQUAKE

#### 3.1. PARAMETERS

The parameters of this earthquake are displayed in Figure 1<sup>[2]</sup>. About 20 miles of the San Andreas fault ruptured. The epicenter was 9 miles north-east of Santa Cruz at a depth of 11.5 miles. The linear accelerator is 32 miles from the epicenter. The magnitude is listed at 7.1 .

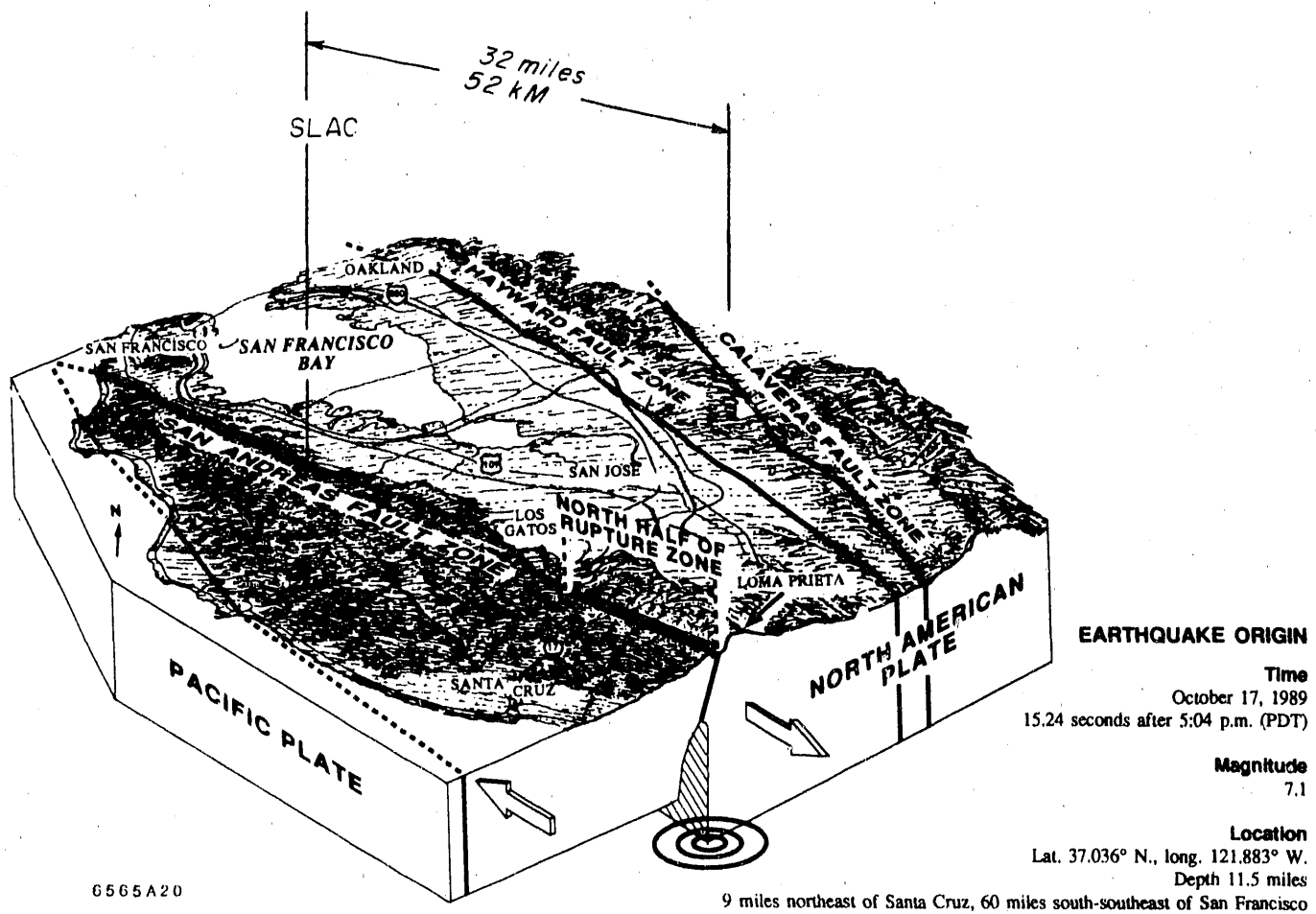


Figure 1. Parameters of the Loma Prieta Earthquake, (from USGS)

### 3.2. THE EVENT WAS FORECAST

By observing the long-term slip rate of a fault and dividing this value into the geodetically determined slip associated with the last major earthquake one can, assuming linear behavior, calculate a return period for the event. The probability of such an event occurring in a given time, is then simply the fraction of the time used up following the last time the event occurred. What makes this field of study so notoriously difficult is that the long term slip rate and the effective slip are very difficult to measure. Moreover values vary dramatically for various regions of ground along the fault. Nevertheless the location and magnitude of the Loma Prieta event was fairly well forecast<sup>[3]</sup>.

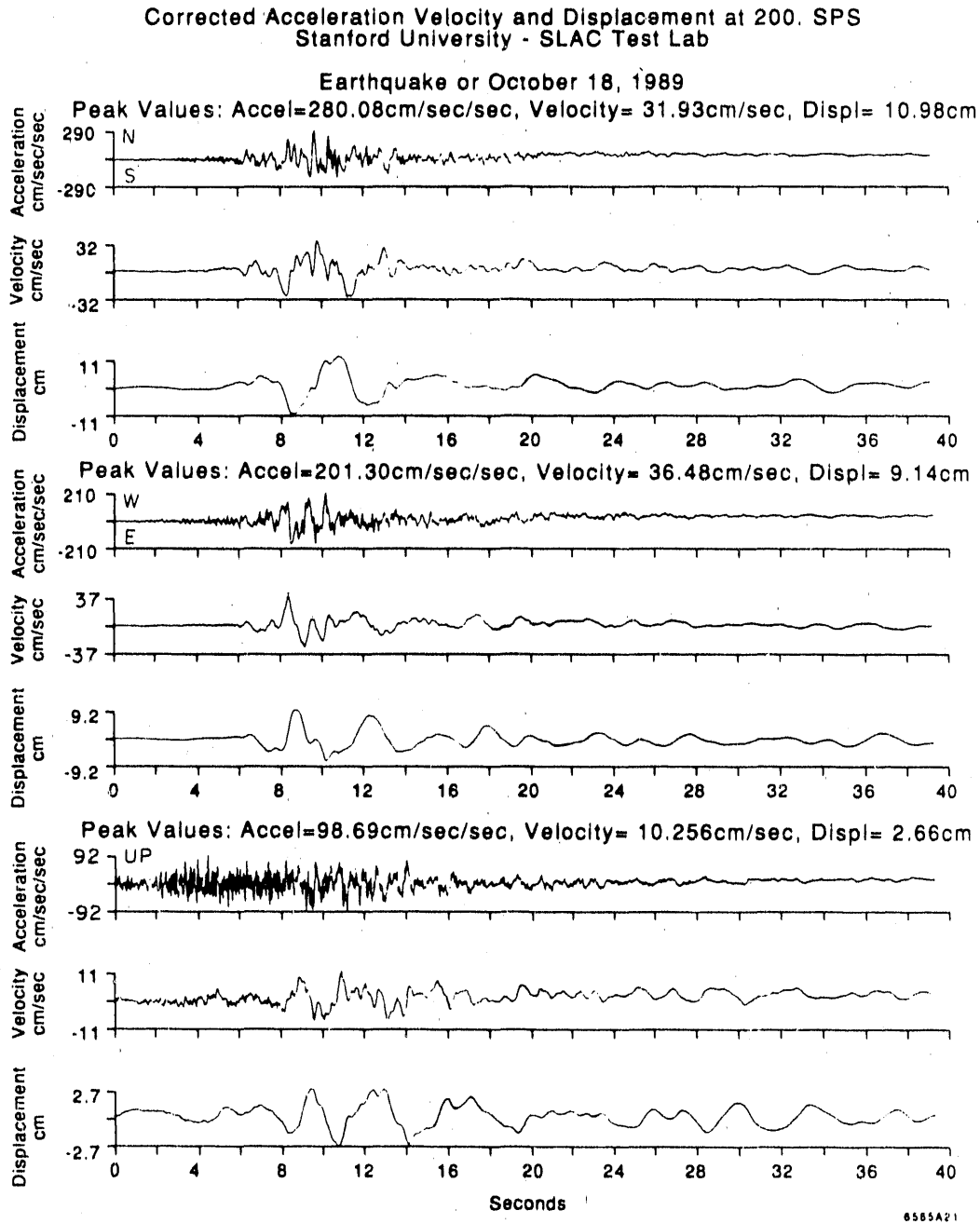
### 3.3. ACCELEROMETER RECORD AT SLAC

Two self triggering strong motion accelerometers were installed on the SLAC site in 1982. One instrument<sup>[4]</sup> was meant to provide a free-field reading, that is unencumbered by nearby man-made structures. This instrument was not in operation at the time of the earthquake. A second instrument was located on the floor against the east wall of the high bay of the test lab (Building 044). The location was chosen to be right on top of the so called "test lab fault". Figure 2 depicts the acceleration records from the test lab instrument. This data was corrected for instrumental response, digitized and integrated with respect to time to provide velocity and displacement values<sup>[5]</sup>. Peak recorded accelerations are 0.29g N and 0.21g W. Notice the peak dynamic amplitudes of 11 cm N and 9 cm W! The three largest horizontal displacement bumps are almost in phase and are along a SW/NE direction, coincidentally *parallel* to the direction of test lab fault. One may also note that although the instruments cannot measure a DC component, there appears to have been more motion (slip?) to the west than to the east during the event.

### 3.4. PEAK ACCELERATIONS RECORDED VS. DISTANCE FROM THE EPICENTER

Peak ground accelerations to be expected in an earthquake are of great importance in the design of earthquake resisting structures<sup>[6]</sup>. Over the past two decades great strides have been made, not only in design, but as greater regions of California became better instrumented, also in a much better ability to separate two dominant variables in the problem; namely (a) local soil conditions and (b) distance from the epicenter. Since the Loma Prieta event occurred almost in SLAC's back yard, it might be interesting to plot peak ground acceleration versus

Figure 2. Records of Corrected Acceleration, Velocity, and Displacement From the Instrument Located in the Test Lab.



epicentral distance for this earthquake. Fortunately, the data are readily available<sup>[7]</sup>. Figure 3 depicts the results; in which the square points denote maximum horizontal (either NS or EW) accelerations observed, plotted as a fraction of the acceleration due to gravity "g".

In those cases in which the data exceeds "rock station" values, *the station was located on less competent ground*. Notice, in particular, the amplification for those stations in Bay Mud. Such poor material is deemed responsible for the substantial damage that occurred in the Marina district of San Francisco (amplification as high as 15) and the collapse of the I-880 structure in Oakland. Two stations are labelled as sitting on granite. Not surprisingly, they suffered accelerations less than those predicted by the curves.

Curves, such as are displayed on Figure 3, should not be taken too seriously. They may be used as a design guide — not as a well founded prediction of what will happen in any given event for several reasons. Among these are: The effects of local strata and those along the motions' flight path cannot be predicted in advance. Data from points having epicentral distances less than the length of the rupture are not only scarce, they are in the *near-field* of the radiating source.

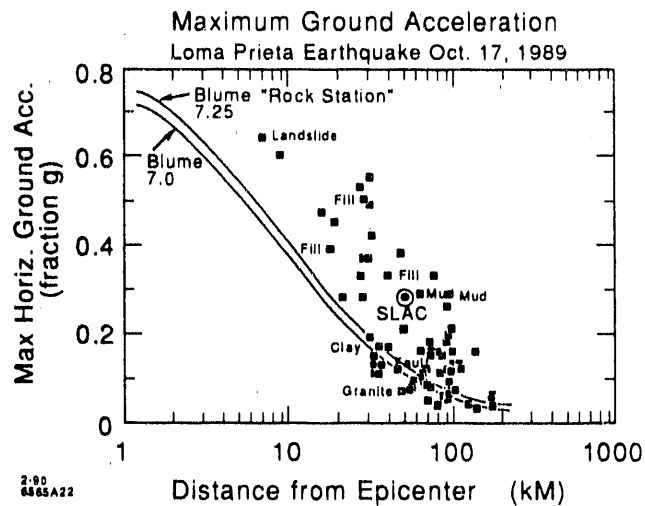


Figure 3. Measured Maximum Horizontal Ground Accelerators vs. Distance From the Epicenter

Nevertheless one cannot help but wonder why the acceleration measured by the instrument in the SLAC test lab is so high. We suspect that these readings to be higher than those to which the accelerator housing or the SLC experimental pit (sited primarily on miocene rock) were subjected to.

## 4. RECENTLY OBSERVED DISPLACEMENTS

### 4.1. GROUND MOTION ALONG THE LINAC

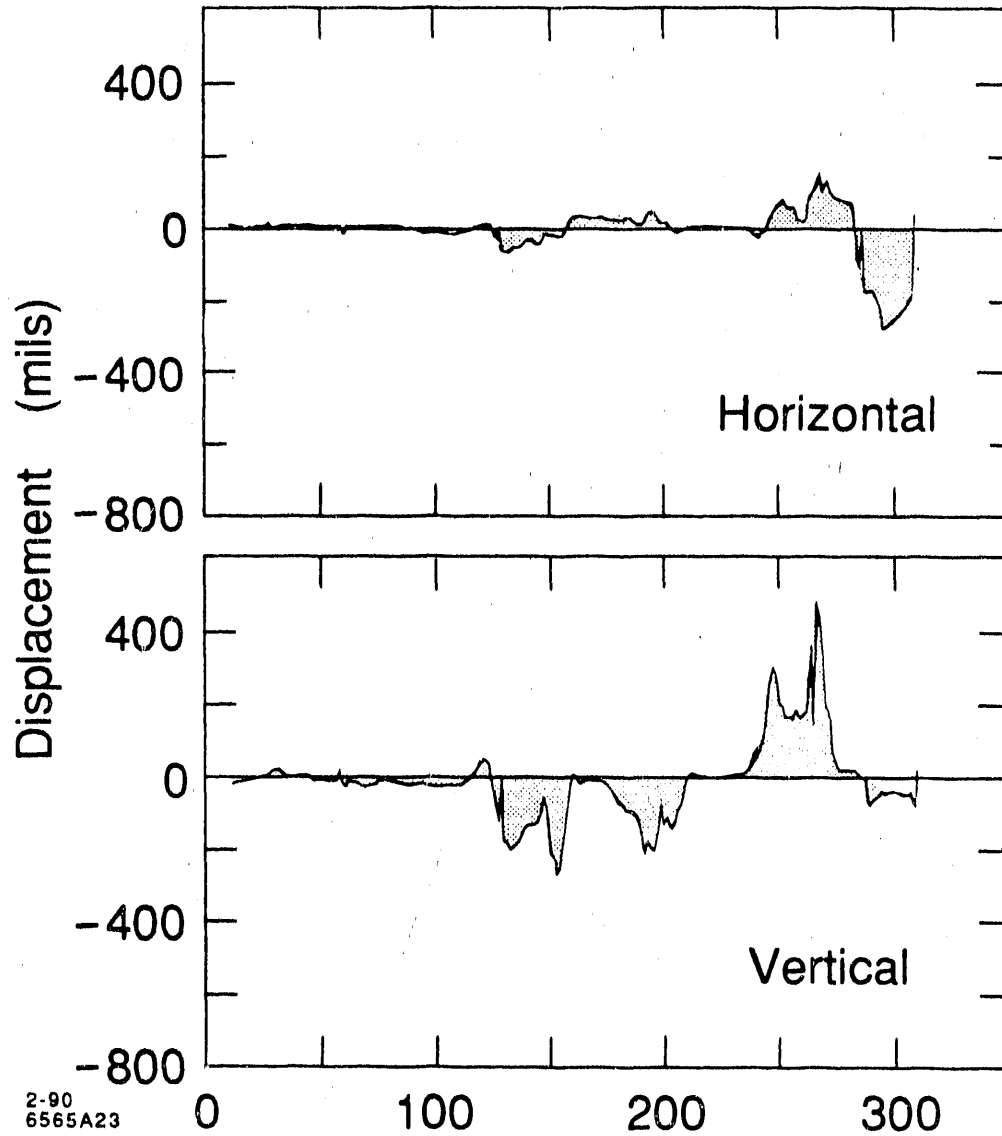
The SLAC laser alignment system<sup>[6]</sup> has been used since 1966 to measure transverse displacement of the linac with respect to a line drawn through two (more or less arbitrarily defined) reference positions (which may themselves be moving with time). Each linac sector (there are 30 in 10,000 ft) generally consists of eight 40 ft support girders, each of which houses a lens station. There are, therefore, (including a number of auxiliary stations) almost 300 lens positions that can be monitored along the 2 mile stretch. For historical reasons the ordinate is plotted in units of 0.001 inches, the abscissa in "station number" in which, for example sector 22 girder 5 would be plotted as station 225. For the vertical scale, positive values mean up. For the horizontal values, positive means motion to the south!

As luck would have it, a complete laser realignment of the linac had been carried out as recently as Oct 3, just two weeks prior to the event. Figure 4 depicts the difference between this data and that taken on Oct 25th seven days after the event. The solid line denotes horizontal displacement, the crosses vertical. The scales of the two graphs have been chosen to be identical. Several features become evident:

- The pattern of downward displacements that occurred from the earthquake in the fill regions (in sectors 12, 13, 14 and 18, 19) is almost identical to the pattern of long term motion as shown in Figure 5 which depicts the cumulative motion of the tunnel (defined to be negative of cumulative corrections applied to keep the linac straight) between the years 1966 and 1983.
- Similarly the pattern of vertical heave in sectors 24, 25, 26 is identical to that observed in long term motion. In magnitude the tunnel appears to have aged in 15 seconds an amount approximately equivalent to 15 years!
- In contrast, very little motion (vertical or horizontal), is seen along the western end of the accelerator, (sectors 0 through 11).
- Most important the tunnel slipped approximately 7 mm to the north starting in the region between stations 28-1 and 28-5 or linac coordinates 90+00 and 91+62. One need hardly comment that this is just where the "test lab

# LINAC Alignment Data

Difference Oct 25th Oct 3rd 1989

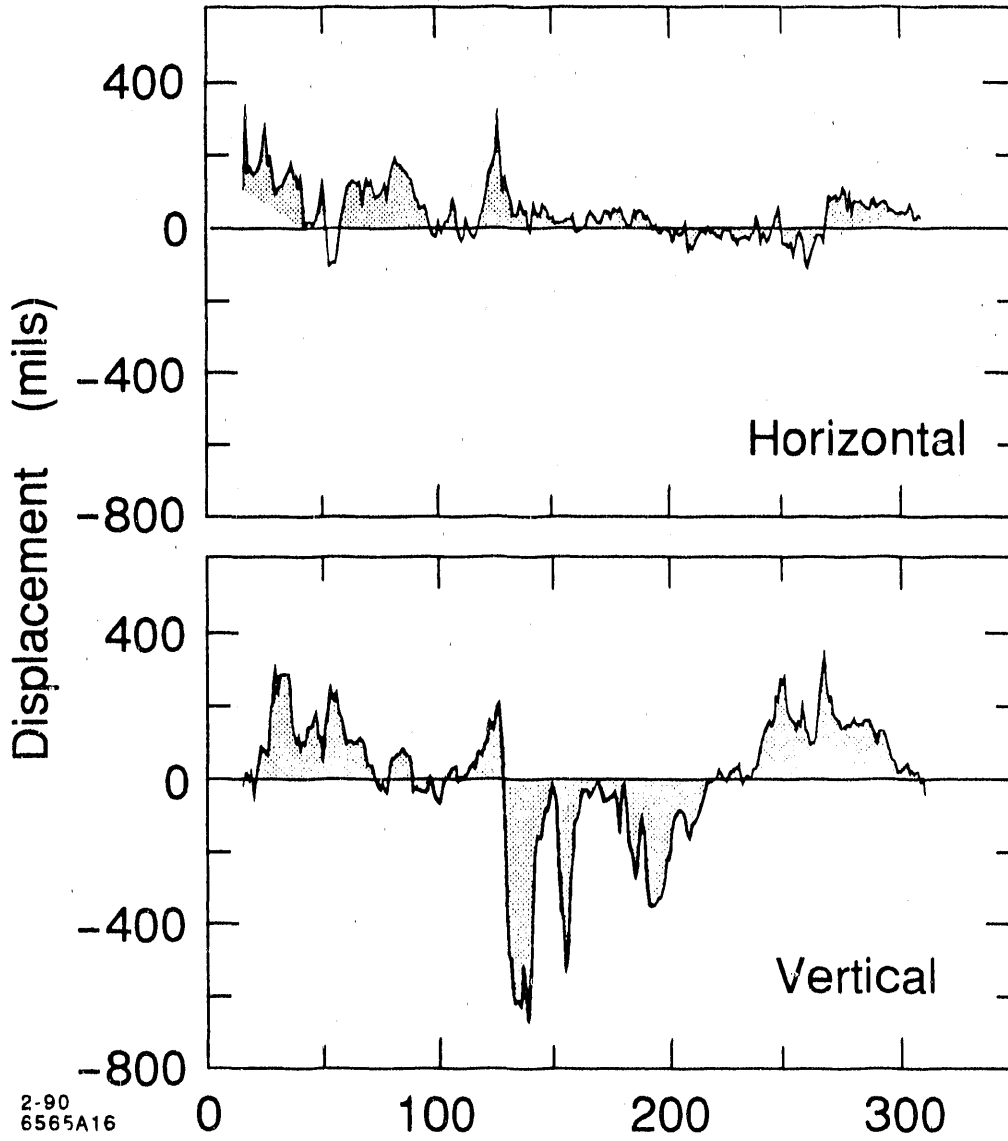


2-90  
6565A23

Figure 4. Displacement of Linac Tunnel Between October 3rd and 25th, 1989

# LINAC Alignment Data

Cumulative Difference: 1983 - - 1966



2-90  
6565A16

Figure 5. Cumulative Linac Tunnel Displacements  
Between 1966 - 1983

fault" crosses the accelerator housing. This motion was large enough that new cracks appeared in the housing wall and that the main laser had to be repositioned. Sectors 24, 25, 26 slipped south by about 2mm. We do not know exactly where the remaining downstream portion of the BSY housing ended up. We must still tie the BSY laser alignment into the main linac system in a rigorous way.

- Lesser horizontal motions ( $\approx 1\text{mm}$ ) occurred in the fill zones.

Realignment measures taken in November 1989 to restore the linac to immediate operation are described by Adolphsen et al.<sup>[9]</sup>.

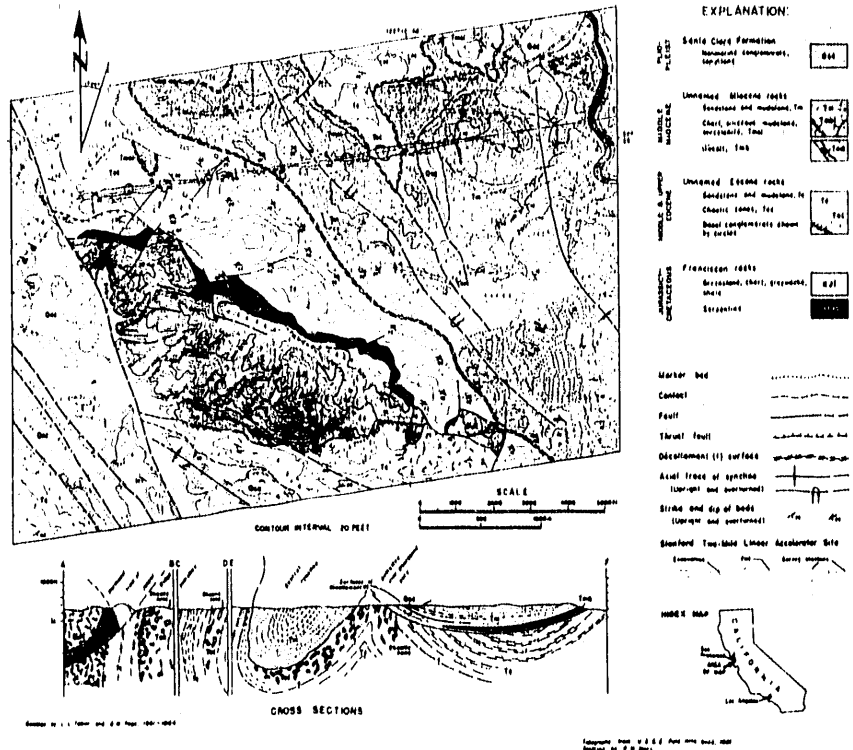
#### 4.2. CORRELATION WITH GEOLOGIC FEATURES ALONG THE LINAC TUNNEL

The excavation for the housing of the two mile long linear accelerator afforded geologists the best exposed cross section of Cenozoic (an age, including the present, during which mammals developed) rocks between the San Andreas fault and San Francisco Bay. The geology and physical properties of the site were studied during 1961-64 in an elaborate program of geologic mapping, boring, trenching, soil testing and measurement of ground movement<sup>[10][11]</sup>.

Figure 6 depicts a cross-section which shows ... "orderly Eocene sandstone, mudstone sequences interrupted by chaotic zones consisting of disordered mudstone with scattered and rotated bodies of sandstone." It was believed that the chaotic structure resulted in part from Eocene submarine sliding, although thrusting of the San Andreas fault system, had it been active in Eocene times ( $>50$  MY, provides an alternative explanation. After the Eocene rocks were moderately folded, Miocene (10 MY) strata were deposited unconformably upon them. Continued thrusting and folding produced a surface of décollement which itself increased the structural complexity of the chaotic zones, in places producing locally overturned intact strata. This process is thought to be responsible for the principal features of the site and produced the hills (cut regions of the tunnel) and valleys (fill regions of the tunnel). In an oversimplified way one can say that with time and shaking, the fill regions sag and the cut regions rebound.

No less than 10 demarcations of regions containing differing species of rock intersect the tunnel. Although these regions are called faults, in this connection this term is used to mean... "that in these areas there were zones of earth movement in the distant geologic past but there has been no discernible movement in historic time". Indeed laser alignment data taken over the past 20 years and after the recent earthquake tends to confirm this statement.

The reports of the 1960's also single out a shallow "bedding plane fault" (shown in Figure 7) between the Miocene deposits and the much more recent poorly consolidated fluvial conglomerate (Plio-Pleistocene age,  $\approx 1$  MY) named Santa Clara

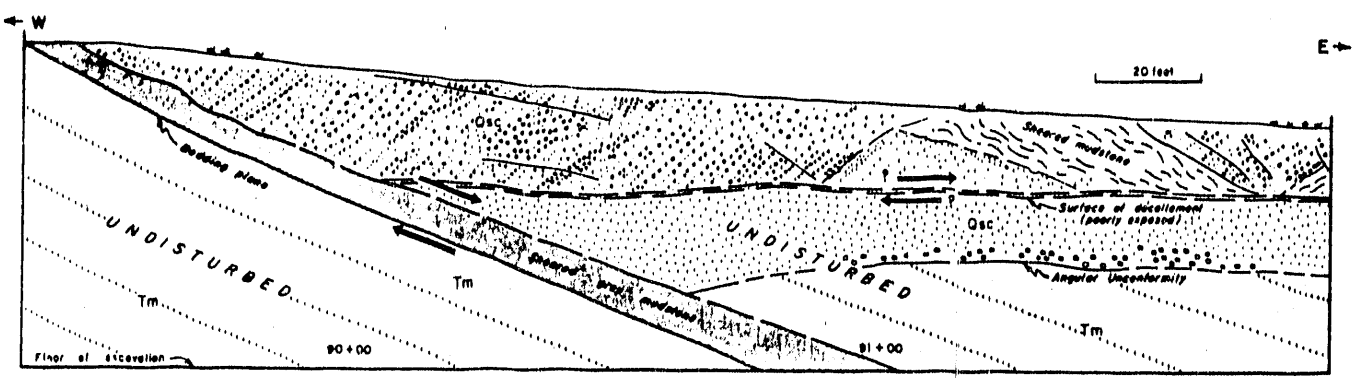


GEOLGIC MAP OF AREA WEST OF STANFORD UNIVERSITY, CALIFORNIA  
 (Geology by Page and Tabor, 1911-1912; topography from U.S. Geological Survey Paleogeographic, 1911; drafted by P. M. Mary)

PAGE AND TABOR, PLATE I  
 Geological Society of America Bulletin, volume 71

6555A1

Figure 6. Geologic Map of the SLAC Site

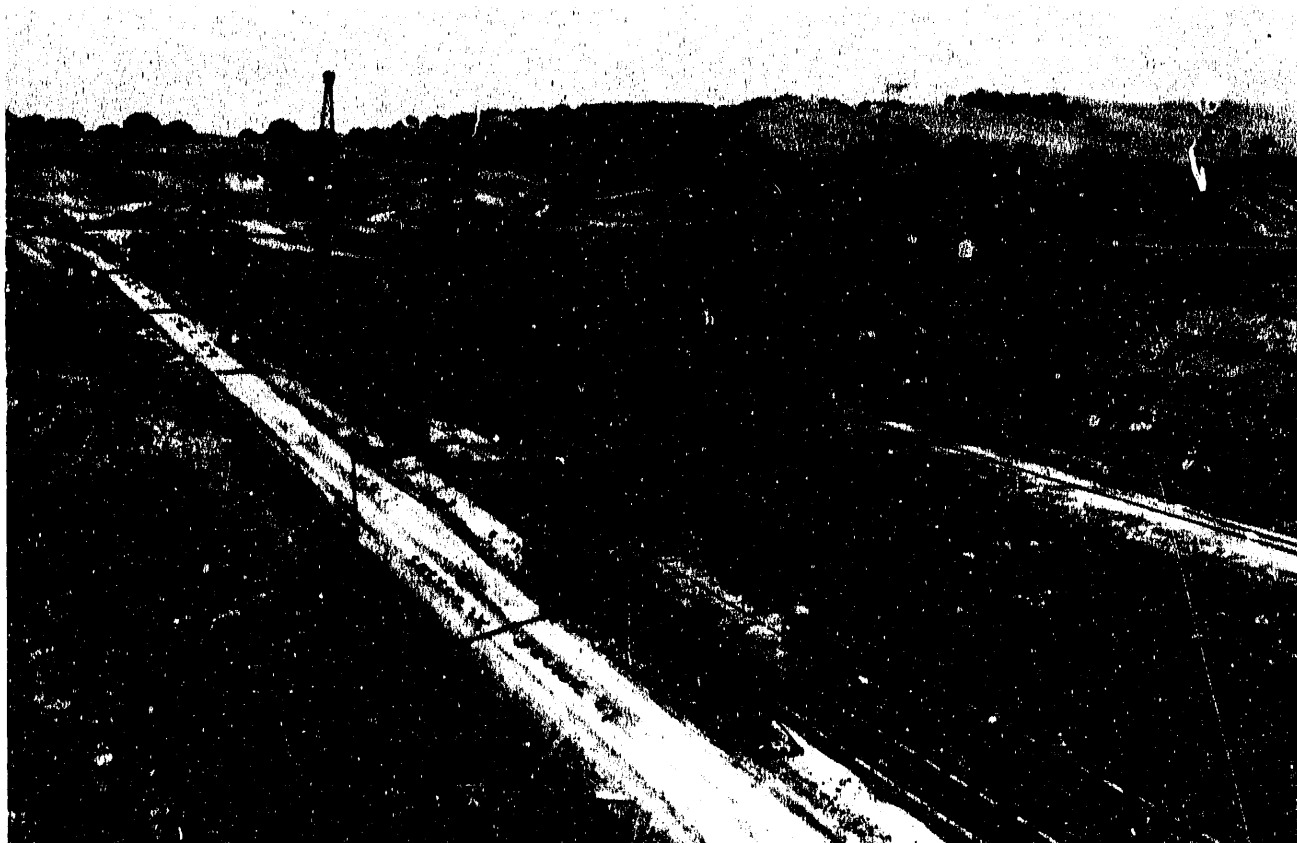


Décollement involving Pliocene-Pleistocene rocks. Horizontal conglomerate of Santa Clara Formation (Qsc) rests unconformably on Miocene beds (Tm). Tilted and jumbled Santa Clara beds have slid on ill-defined décollement surface. Fault parallel with Miocene beds has offset earlier structures. (Side of linear accelerator excavation near station 91+00. View has been reversed from actual exposure, so observer is looking in about the same direction as in Figure 4. Vertical scale is same as horizontal scale.)

6555A3

Figure 7. From Page and Tabor op.cit.

Formation. This ten-foot-thick layer of sheared mudstone intersects the accelerator tunnel around station 91+00 precisely where the 7mm break occurred during the earthquake. It is also called the "test lab fault" because it manifests itself under that building. Figure 8 is a photograph of the fault taken in 1964.



6665A4

*JUN 12 1964*

Figure 8. Photograph of the Fault Taken During Construction

Before leaving the linac it should be mentioned that there exists another correlation between slow tunnel motion and the site parameters. By 1971 sufficient data had been accumulated using the laser alignment system to draw definite conclusions about the effect of ground water levels in the "fill" area of sector 13. The seasonal correlations shown in Figure 9<sup>[12]</sup> are quite dramatic. Such local deformations make the study of tectonic strain of the near by San Andreas fault system

quite difficult.

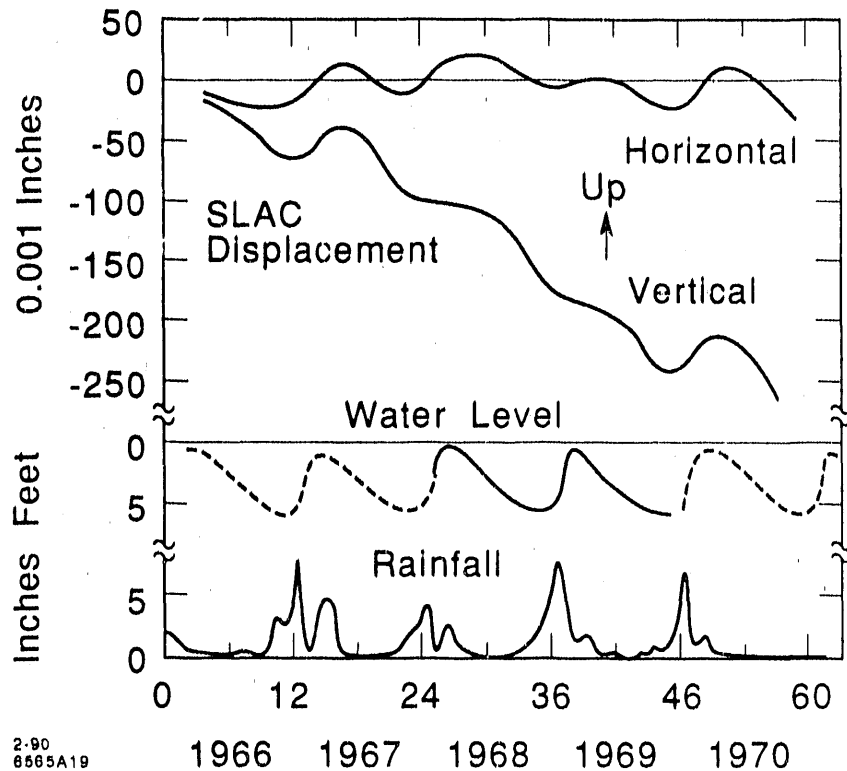


Figure 9. Seasonal Motions Correlated with Rainfall and Ground Water Levels

#### 4.3. GROUND MOTION AT THE STORAGE RING PEP

An elevation survey of the tunnel floor of this 2.2km circumference ring taken with the Hydrostatic Level System<sup>(13)</sup> is shown in Figure 10. The values plotted represent changes with respect to the most recent data set taken prior to the earthquake in 1987. The deviations are large. Movements in prior years were generally at the rate of 1/2 to 1 mm/year. One might expect some vertical weakness at locations where the PEP tunnel passes above the SLC tunnels. In the south this occurs almost in the middle of PEP IR-6 and is probably masked by the hall. On the north a dip is seen just west of IR-12 which coincides with the tunnel crossing. It is difficult to interpret the overall shape of the results except to note

a pronounced discontinuity centered on IR-10. Interestingly a discontinuity is also evident in the radial (horizontal) resurvey of the floor monuments shown in Figures 11a, b, c at the same location, namely halfway between IR-10 and the symmetry point of arc 11. Clues to the explanation of these observations may be found in the following section.

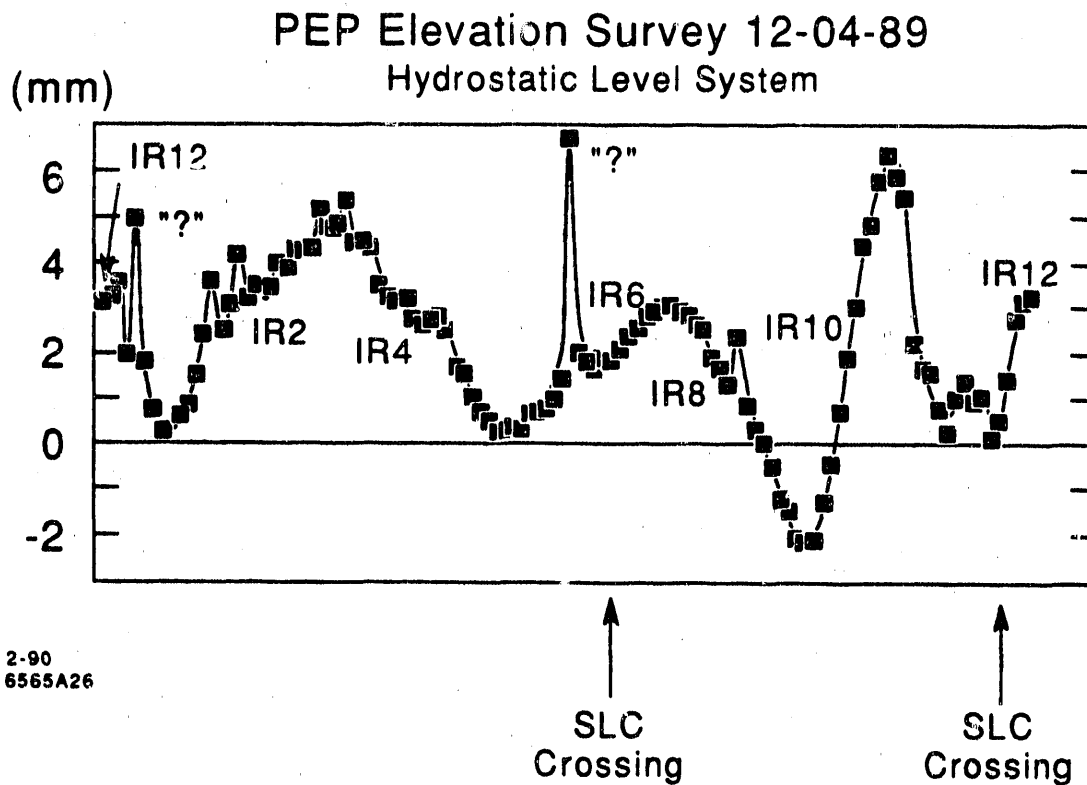


Figure 10. Hydrostatic Level Survey of PEP Tunnel, Differences in Elevation Between 1987 and Dec., 1989

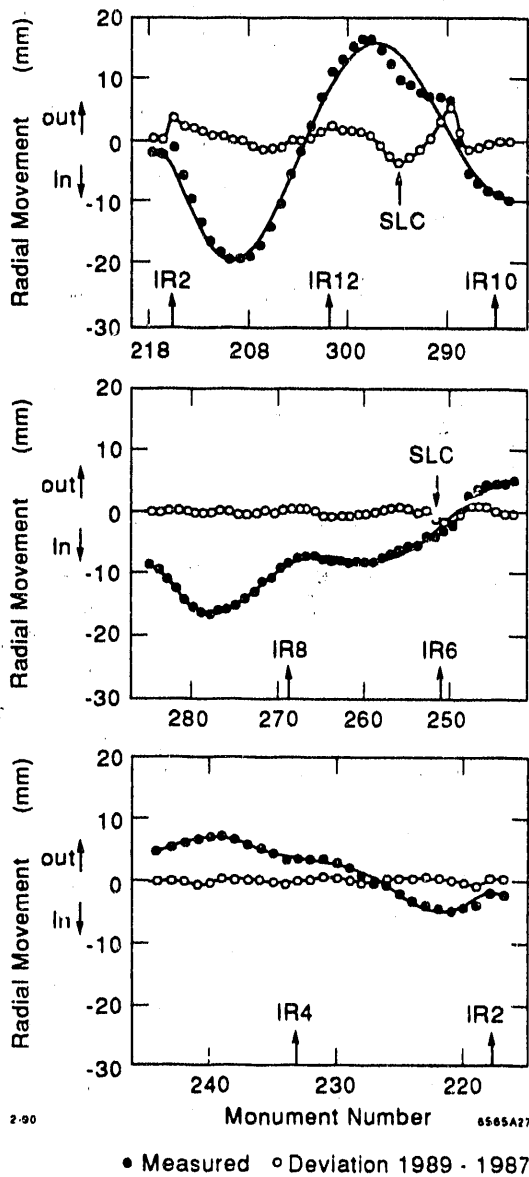


Figure 11. Horizontal Survey of PEP Floor Monuments, December 1989

#### 4.4. GEOLOGIC DETAIL FOR THE CONSTRUCTION OF THE PEP TUNNEL

The early history of geologic investigations regarding the PEP site is described by Bob Gould<sup>[14]</sup>. The work done by Tabor, Earth Sciences Associates of Palo Alto, and the results of an intensive summer 1975 drilling program are chronicled. Among the various problems that were described, the situation in PEP-Region 11 is relevant today. Lenses of siltstone in clay matrix were found in the miocene of borehole 11-1. Slickensided surfaces and scaly clay were abundant throughout the 10 ft thickness of this material.

The detailed geotechnical report for the architect-engineering firm PBQ&D, Inc./Kaiser Engineers for PEP construction was written by the firm Dames and Moore<sup>[15]</sup>. The suspect region is described as: "A very plastic claystone unit is present as an interbed in the vicinity of station 19+00 ... The rock is characterized by a tendency to swell and demonstrates a loss of strength with time when unconfined and exposed to water" and ending with: "special tunnel design and construction should be applied in this vicinity". Plate 2 (of 8 Plates) from this report provides high detail of the PEP bedrock geology in this region.

#### 4.5. GROUND MOTION IN THE SLC NORTH ARC

Figure 12a shows an apparent 12 mm horizontal discontinuity in the 1.1 km long north SLC arc magnet system just upstream of the north reverse bend section. Survey teams were led to this point because the electron beam could not be transported past this region. Figure 12b shows that the magnets have also slipped vertically at this point. To check that it was the floor that moved rather than the magnet supports, a vertical check of floor rivets was performed. The results of this measurement are shown in Figure 13. The break appears to occur at the entrance to achromat 8A at a point 1325 feet in the arc "s" coordinate, ie. from station linac 100+00 in the Beam Switchyard.

#### 4.6. GEOLOGIC INVESTIGATIONS OF THE SLC SITE

Earth Science Associates (ESA) under subcontract to the A and E firm for SLC, the Tudor Engineering Company of San Francisco carried out the geotechnical investigations of the SLC site. Their final work can be found in the Contract Drawings<sup>[16]</sup>. On plate 2 one may note (at about 9:30 o'clock along the tunnel route) the entry "strike slip movement" indicating a fault first identified by Tabor in the early 60's on Map 9 (Target Area) in ABA-88. This fault, described as a "pinch and swell structure containing gaugy dark grey-blue clay with slickensides" can still be seen with the naked eye in the cut of the road to SPEAR as a marked

indentation in the grass just under SSRL Building No 288. Also shown is the clay lens found in PEP Bore hole 11-1 and 11-4 projected to the SLC tunnel. The possibility of this lens causing mischief during SLC tunneling must have given rise to the drilling of SLC-12. When no clay was found, this possibility was removed and is therefore not shown on the geologic contract drawing.

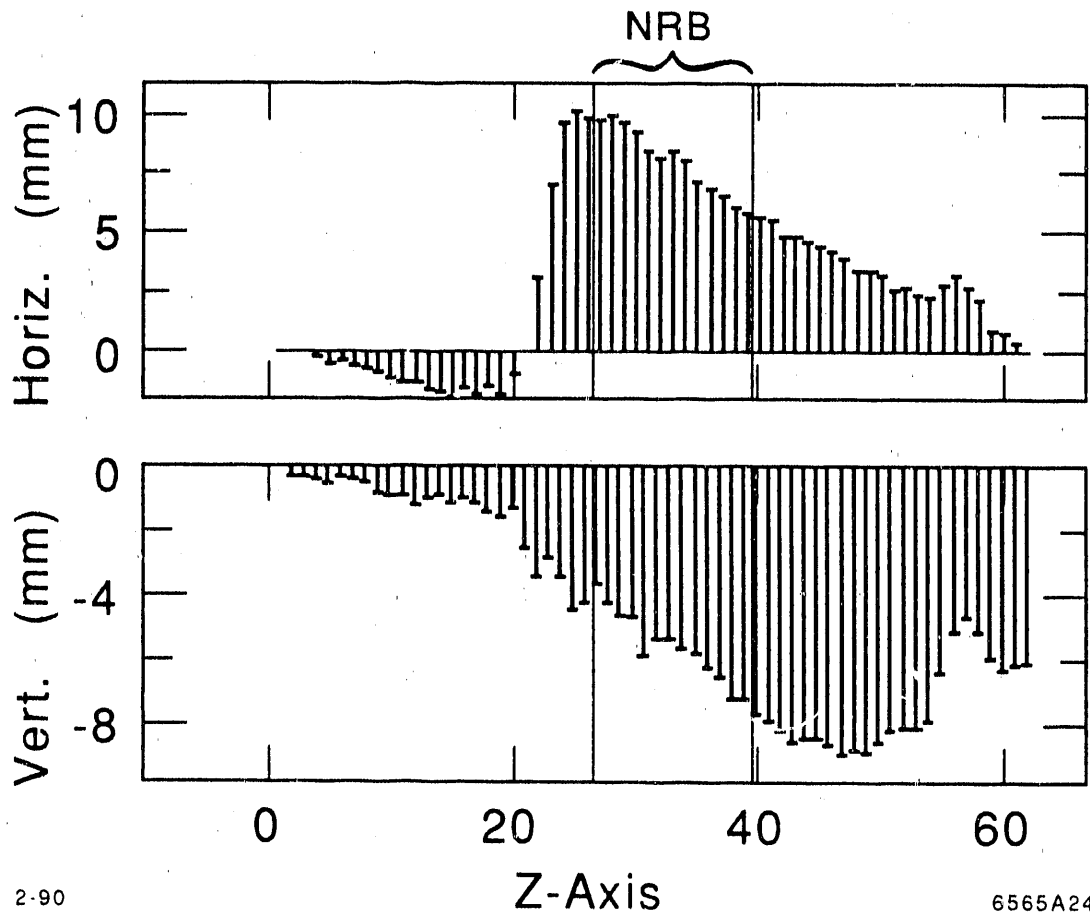


Figure 12. Horizontal and Vertical Discontinuities in North Arc in Achromat 8a

Although it is tempting to associate the north arc discontinuity with the fault found by Tabor, the coordinates simply do not match. The fault is at 1100 to 1200 ft and the discontinuity occurs at 1325 ft. It is interesting to recall that the tunneling contractor found a 3 - 5 gpm water inflow at  $s = 1325$ ft. Such flows were noted also in other places but there were no indications, in contrast to

other problem areas where swelling stone was encountered, in the inspectors logs of unusual geology.

### Elevation Differences After Earth Quake (10 times magnified)

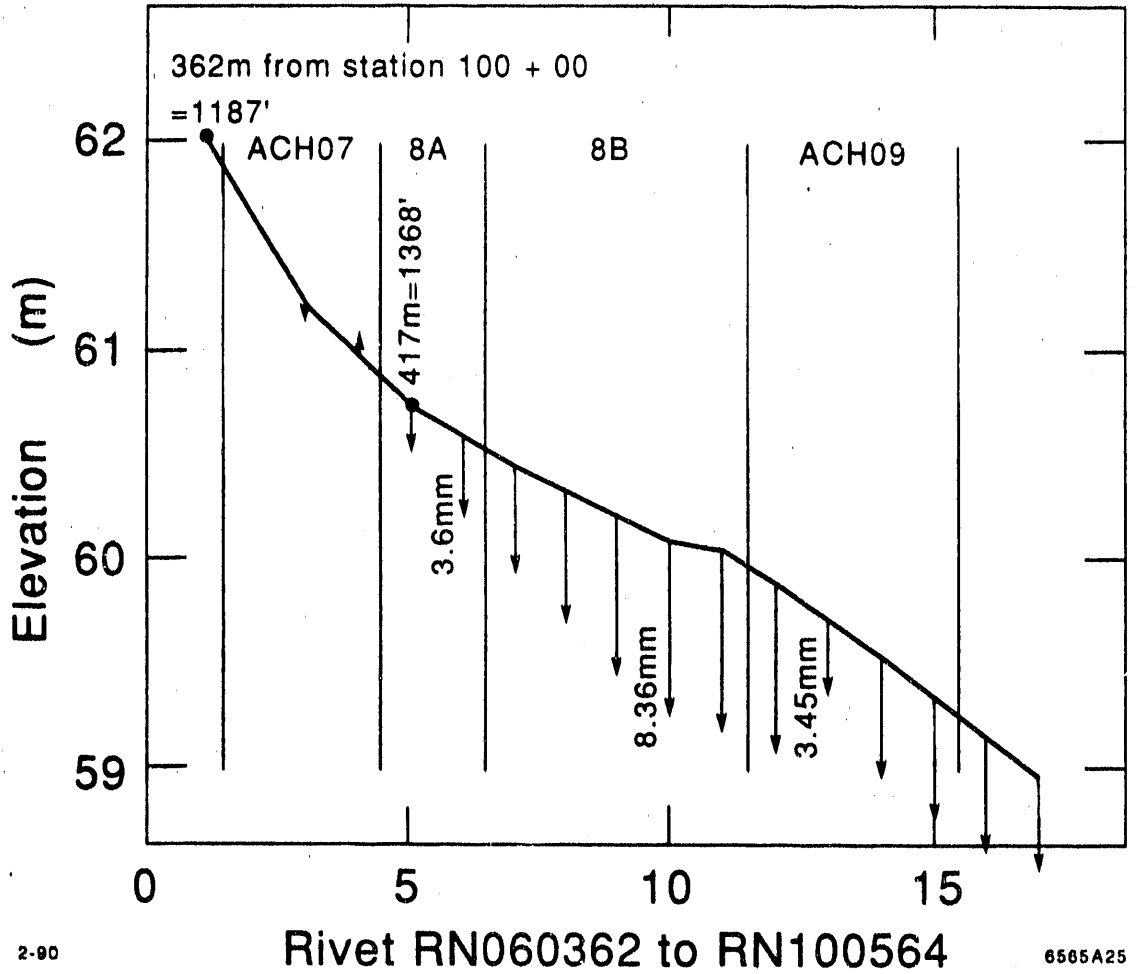


Figure 13. Vertical Survey of Floor Elevation Rivets Near Achromat 8

Our interpretations of these facts are: The water probably runs along the clay lens found at PEP. This lens is oriented toward the SLC tunnel but does not intersect it. The earthquake moved the ground parallel to the slip plane of the lens and the nearby tunnel with it. This explanation appears plausible but no "smoking gun" has yet been found to substantiate the hypothesis. It is interesting to note that so far no other major discontinuities have appeared in the arcs large enough to stop the beam. Certainly other regions possess more suspect geologies. Only a complete resurvey (apparently not warranted at this time) might detect such places.

## 5. MOTION OF EQUIPMENT RELATIVE TO THEIR HOUSING

In general, beam dynamics considerations dominate placement tolerances of components in the plane *transverse* to the particles' motion. For this reason great care is exercised in the mechanical design of the mountings to provide rigid, high resolution and reproducible adjustments in this plane. Perhaps less attention is paid to constraints in the axial direction. Although vacuum integrity was nowhere compromised, we discuss in this section three areas in which the earthquake produced effects which may require more attention in the future.

### 5.1. THE LINAC ALIGNMENT SYSTEM LIGHT PIPE

The copper waveguide of the accelerator proper is supported on some 240 strongback girders, each 40 ft long consisting of 2ft diameter hollow aluminum tube. These tubes are connected with each others ends by means of 24" diameter, 2" long vacuum bellows to permit their evacuation while allowing for thermal expansion. Mounting to the floor and side wall of the tunnel is shown in Figure 14. Axial restraint is by means of a brace per girder to the wall as shown. The brace fasteners are held to unistruts imbedded in the wall by dogs that resist shear forces through friction. During the earthquake, considerable longitudinal waves must have been set up in the structure which has all the properties of a mechanical delay line. Judging by scrapes on the paint between the wall and mounts, amplitudes up to  $\pm 0.75$  inches appear to have occurred. Most stations moved between  $1/8$ " to  $1/4$ ". Eight sections did not return to their equilibrium positions. Vacuum bellows problems also occurred at the accelerating waveguide itself. Some 16 focusing magnets had to be opened to repair these problems.

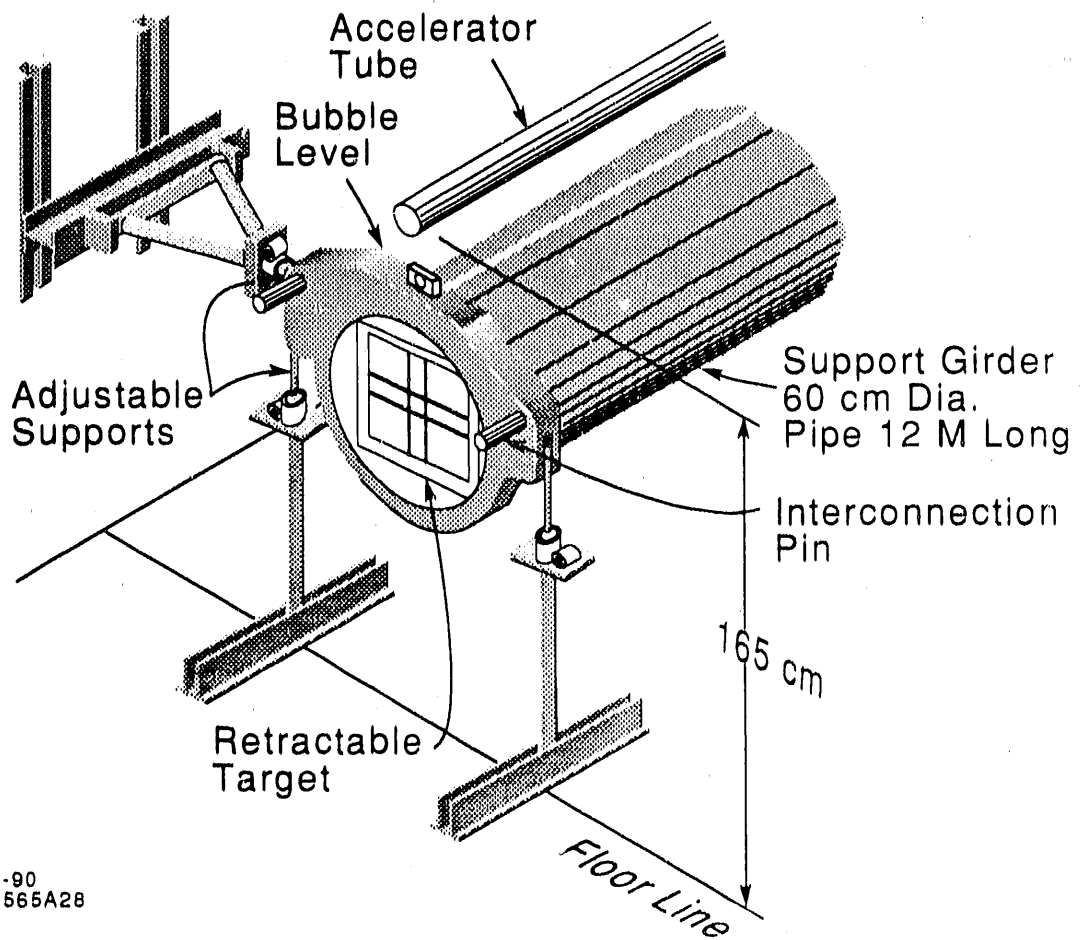


Figure 14. Method of Support - Linear Girder

**Physical description**  
 Base-isolation is a design strategy founded on the premise that a structure can be substantially decoupled from damaging horizontal motions of earthquake ground motion. The result is a structure that is isolated from the level of forces and accelerations to which the structure is subjected.

Use of the concept of base isolation has recently become a practical reality with the development of lead-rubber bearings. These isolated bearings exhibit flexible ductile behavior when subjected to severe earthquake motions and thus provide both dynamic decoupling and energy dissipation. The result is a structure that is isolated from ground motion and a vertical load support are contained within a single component.

Extensive research has confirmed the effectiveness of lead-rubber bearings in the research environment to become a viable practical concept.

Lead-rubber bearings can be incorporated into the design of both new structures and existing structures. The bearings have already been used in a number of building and bridge structures in seismic areas. Base-isolation incorporating seismic areas. Base-isolation incorporating new two-story buildings, between new bridges and live existing bridges in New Zealand. They are also being used for the seismic retrofit of a bridge for the California Department of Transportation. The system is also

**Physical description**  
 The physical construction of a typical lead-rubber bearing (see Figure 1) consists of the following components:  
 - Alternating rubber layers and thin steel plates are bonded together to form a unit which is subjected to vertical loads.

**Physical description**  
 The physical construction of a typical lead-rubber bearing (see Figure 1) consists of the following components:  
 - Alternating rubber layers and thin steel plates are bonded together to form a unit which is subjected to vertical loads.

**Physical description**  
 The physical construction of a typical lead-rubber bearing (see Figure 1) consists of the following components:  
 - Alternating rubber layers and thin steel plates are bonded together to form a unit which is subjected to vertical loads.

**Physical description**  
 The physical construction of a typical lead-rubber bearing (see Figure 1) consists of the following components:  
 - Alternating rubber layers and thin steel plates are bonded together to form a unit which is subjected to vertical loads.

**Physical description**  
 The physical construction of a typical lead-rubber bearing (see Figure 1) consists of the following components:  
 - Alternating rubber layers and thin steel plates are bonded together to form a unit which is subjected to vertical loads.

**Physical description**  
 The physical construction of a typical lead-rubber bearing (see Figure 1) consists of the following components:  
 - Alternating rubber layers and thin steel plates are bonded together to form a unit which is subjected to vertical loads.

**Physical description**  
 The physical construction of a typical lead-rubber bearing (see Figure 1) consists of the following components:  
 - Alternating rubber layers and thin steel plates are bonded together to form a unit which is subjected to vertical loads.

**Physical description**  
 The physical construction of a typical lead-rubber bearing (see Figure 1) consists of the following components:  
 - Alternating rubber layers and thin steel plates are bonded together to form a unit which is subjected to vertical loads.

**Physical description**  
 The physical construction of a typical lead-rubber bearing (see Figure 1) consists of the following components:  
 - Alternating rubber layers and thin steel plates are bonded together to form a unit which is subjected to vertical loads.

**Physical description**  
 The physical construction of a typical lead-rubber bearing (see Figure 1) consists of the following components:  
 - Alternating rubber layers and thin steel plates are bonded together to form a unit which is subjected to vertical loads.

**Physical description**  
 The physical construction of a typical lead-rubber bearing (see Figure 1) consists of the following components:  
 - Alternating rubber layers and thin steel plates are bonded together to form a unit which is subjected to vertical loads.

**Physical description**  
 The physical construction of a typical lead-rubber bearing (see Figure 1) consists of the following components:  
 - Alternating rubber layers and thin steel plates are bonded together to form a unit which is subjected to vertical loads.

**Physical description**  
 The physical construction of a typical lead-rubber bearing (see Figure 1) consists of the following components:  
 - Alternating rubber layers and thin steel plates are bonded together to form a unit which is subjected to vertical loads.

**Physical description**  
 The physical construction of a typical lead-rubber bearing (see Figure 1) consists of the following components:  
 - Alternating rubber layers and thin steel plates are bonded together to form a unit which is subjected to vertical loads.

**Physical description**  
 The physical construction of a typical lead-rubber bearing (see Figure 1) consists of the following components:  
 - Alternating rubber layers and thin steel plates are bonded together to form a unit which is subjected to vertical loads.

**Physical description**  
 The physical construction of a typical lead-rubber bearing (see Figure 1) consists of the following components:  
 - Alternating rubber layers and thin steel plates are bonded together to form a unit which is subjected to vertical loads.

**Physical description**  
 The physical construction of a typical lead-rubber bearing (see Figure 1) consists of the following components:  
 - Alternating rubber layers and thin steel plates are bonded together to form a unit which is subjected to vertical loads.

**Physical description**  
 The physical construction of a typical lead-rubber bearing (see Figure 1) consists of the following components:  
 - Alternating rubber layers and thin steel plates are bonded together to form a unit which is subjected to vertical loads.

**Physical description**  
 The physical construction of a typical lead-rubber bearing (see Figure 1) consists of the following components:  
 - Alternating rubber layers and thin steel plates are bonded together to form a unit which is subjected to vertical loads.

**Physical description**  
 The physical construction of a typical lead-rubber bearing (see Figure 1) consists of the following components:  
 - Alternating rubber layers and thin steel plates are bonded together to form a unit which is subjected to vertical loads.

**Physical description**  
 The physical construction of a typical lead-rubber bearing (see Figure 1) consists of the following components:  
 - Alternating rubber layers and thin steel plates are bonded together to form a unit which is subjected to vertical loads.

**Physical description**  
 The physical construction of a typical lead-rubber bearing (see Figure 1) consists of the following components:  
 - Alternating rubber layers and thin steel plates are bonded together to form a unit which is subjected to vertical loads.

**Physical description**  
 The physical construction of a typical lead-rubber bearing (see Figure 1) consists of the following components:  
 - Alternating rubber layers and thin steel plates are bonded together to form a unit which is subjected to vertical loads.

**Physical description**  
 The physical construction of a typical lead-rubber bearing (see Figure 1) consists of the following components:  
 - Alternating rubber layers and thin steel plates are bonded together to form a unit which is subjected to vertical loads.

**Physical description**  
 The physical construction of a typical lead-rubber bearing (see Figure 1) consists of the following components:  
 - Alternating rubber layers and thin steel plates are bonded together to form a unit which is subjected to vertical loads.

**Physical description**  
 The physical construction of a typical lead-rubber bearing (see Figure 1) consists of the following components:  
 - Alternating rubber layers and thin steel plates are bonded together to form a unit which is subjected to vertical loads.

**Physical description**  
 The physical construction of a typical lead-rubber bearing (see Figure 1) consists of the following components:  
 - Alternating rubber layers and thin steel plates are bonded together to form a unit which is subjected to vertical loads.

**Physical description**  
 The physical construction of a typical lead-rubber bearing (see Figure 1) consists of the following components:  
 - Alternating rubber layers and thin steel plates are bonded together to form a unit which is subjected to vertical loads.

**Physical description**  
 The physical construction of a typical lead-rubber bearing (see Figure 1) consists of the following components:  
 - Alternating rubber layers and thin steel plates are bonded together to form a unit which is subjected to vertical loads.

**Physical description**  
 The physical construction of a typical lead-rubber bearing (see Figure 1) consists of the following components:  
 - Alternating rubber layers and thin steel plates are bonded together to form a unit which is subjected to vertical loads.

Figure 15. Sketch of a Commercially Available Earthquake Isolation Pad

## 5.2. THE ARC MAGNETS

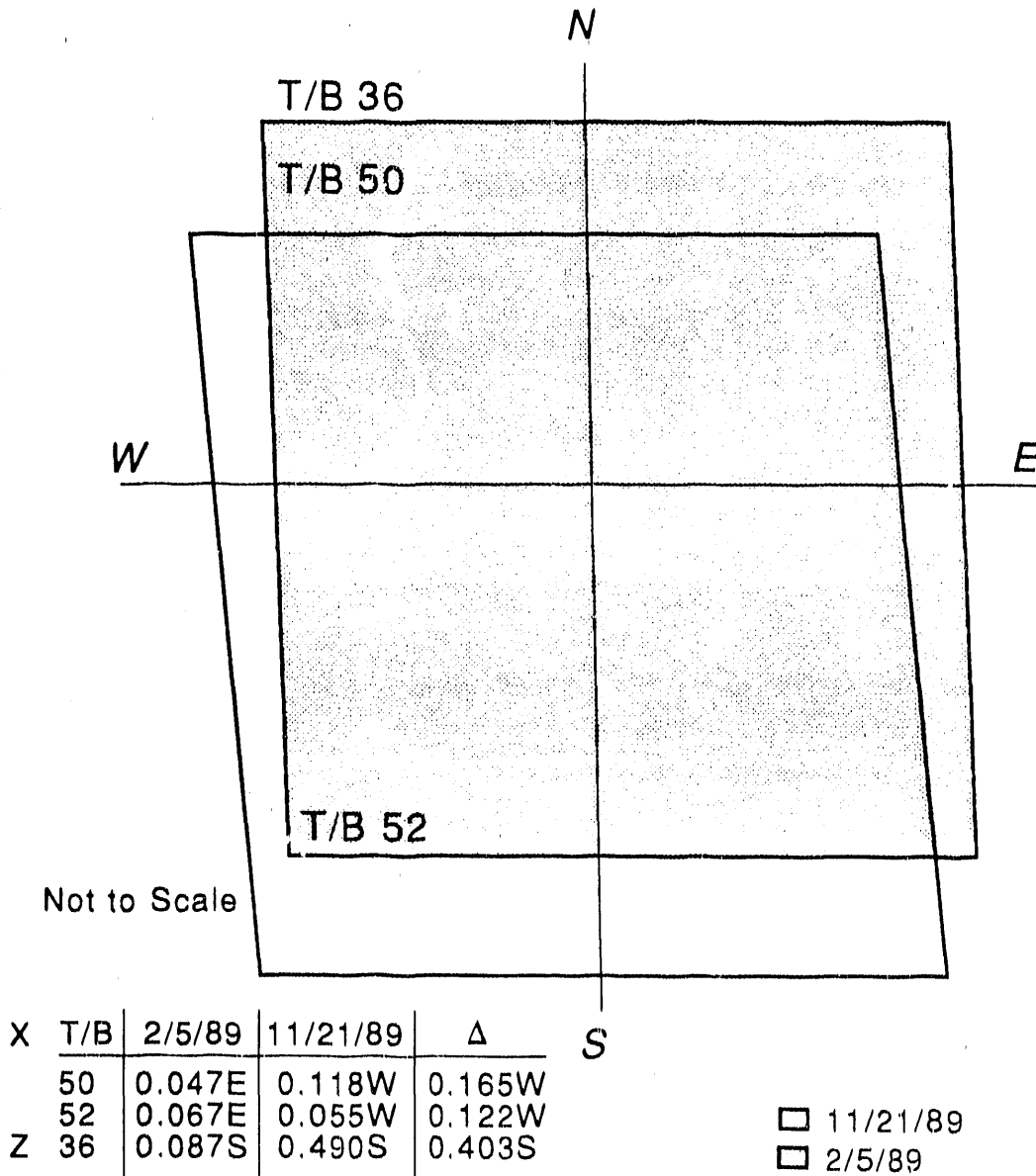
Similar effects occurred in the mounts of the SLC arc magnets. Some mounts were bent so as to move the magnets in the axial direction. In the arcs the situation is aggravated by the fact that the tunnels are not in a horizontal plane, in fact have slopes up to 10%. Axial motions up to 1/2" were sufficient to completely collapse some vacuum bellows. Abnormal conditions were observed in 13 places in south arc achromats 4, 10, 11, 18, 20, 21, 22 and 23. Deformations were also observed in 36 locations of north arc achromats 10, 11, 12, 13, 14, 15 and 16.

## 5.3. THE MARK II DETECTOR

The central portion of the 1800 ton Mark II detector is mounted on four specially designed "Seismic Base Isolators"<sup>(17)</sup> so that it need not be fully braced to the experimental pit walls. Generic versions of the pads are described in Figure 15. Since no damage appears to have been done to the Mark II detector, we infer that the mountings performed as designed. The question arises, with what amplitude did the 1800 tons move relative to the floor during the earthquake? This amplitude is a non-linear function of the peak accelerations applied by the earthquake. Since we do not have a record of the actual acceleration of the collider hall floor we can only set some limits. Let us assume the test-lab recording obtained in the collider hall. From the response curves we obtain a force reduction to 60% for a maximum acceleration of 0.29g. Lesser forces have lesser reductions. Making the drastic assumption that the frequency response is the same (probably unwarranted) one would guess that the Mark II had an maximum amplitude of about 6 cm. Was this possible? Probably not! The central vacuum chamber bellows would have taken up this amount of motion but the bellows protector would have been damaged. Marks on the protector are consistent with only 1/2" motion. After all the motion ceased the detector came to rest about .4" south and .14" west from where it had been before the quake. (See Figure 16). The detector has since been realigned.

# Mark II Positions

Post Earthquake  
Relative to Pre-earthquake Monument Positions



2-90

6565A30

Figure 16. Change in Location of MarkII Detector Due to Earthquake

## 6. CONCLUSIONS

Although additional alignment information will continue to become available in the coming year the following conclusions may be drawn at this time.

- Permanent deformations of the accelerator housing and arc tunnels ( $\approx 1$  cm) appear to have occurred at sharp locations that have either known or suspected geologically recent clay formations.
- Other, more broadly distributed deformations of the linac have occurred in regions that have been traditionally associated with sagging fill or rebound of cuts. The patterns of deformations are the same, the magnitudes ( 1 to 2 cm ) are comparable to slow motions that have been accumulating since construction in the mid 1960's.
- No deformations appear to have occurred at faults which have been considered "geologically inactive".
- We do *not* have unambiguous evidence what accelerations the experimental collider hall and the accelerator housing (in which some of the laboratory's most valuable equipments are located) were actually subjected to. Two new instruments are being mounted to overcome this deficiency.
- Since new rate of drift measurements along known faults as well as increased strain resulting from the recent earthquake have served to *increase* the sum probability of an event in the San Francisco Bay Area to about 67% in the next 30 years, it would seem prudent to begin discussions of cost/benefit evaluations of further earthquake countermeasures over the projected lifetime of the facility. Axial restraints are an example that might be worth looking into.

## 7. ACKNOWLEDGEMENTS

It is pleasure to acknowledge the work of the SLAC survey and alignment teams whose data is summarized above. This summary report is based on an extensive compilation of geologic and alignment data by G.E.Fischer.<sup>[18]</sup>

## REFERENCES

1. Geological Investigation of the Stanford Two-Mile Linear Accelerator Site, F.W.Atchley, R.O.Dobbs, Microwave Laboratory Report No.682 January 1960, page 1-14. see also Appendix III
2. The Loma Prieta Earthquake of October 17,1989, U.S.Geological Survey pamphlet P.L.Ward, R.A.Page et al. 1989
3. Probabilities of large Earthquakes occurring in California on the San Andreas Fault, The working group on California Earthquake Probabilities, USGS OFR - 88 -398, Menlo Park, 1988
4. Made by the Kinometrics Co. 222 Vista Ave. Pasadena CA. 91107
5. These curves were made available through the courtesy of Dr.Gerald Brady, USGS Menlo Park CA. (415) 329-5664
6. See for example: Earthquake Design Considerations for the Accelerator Housing Structures of the Stanford Linear Accelerator Center, by John A. Blume, Report No.2, June 3rd 1963, pages 6-9
7. Report No.0SMS 89 - 06, Office of Strong Motion Studies, Division of Mines and Geology, California Department of Conservation, 630 Bercut Drive, Sacramento, CA 95814
8. Precision Alignment Using a System of Large Rectangular Fresnel Lenses, W.B.Herrmannsfeldt et a. Applied Optics, Vol. 7,p995 (1968)
9. SLC Accelerator Physics Experiment No.115, C.Adolphsen, F.Linker, W.Oren, R.Ruland and J.Seeman, November 21 1989
10. Chaotic Structure and Décollement in Cenozoic Rocks near Stanford University, California. B.M.Page and L.L.Tabor, Geological Society of America Bulletin, v.78, p.1-12 January 1967
11. Geologic Site Investigation for the Stanford Linear Accelerator Center, Report No. ABA-88 March 1965, Aetron-Blume-Atkinson AEC Contract AT(04-3) S 136, unpublished
12. Seasonal Deformations of 2-Mile Straight Line, J.J.Spranza, A.M.Nur, Journal of the Soil Mechanics and Foundations Division, Proceedings of the American Society of Civil Engineers,Vol. 97,No.SM12, December 1971, p. 1623.
13. T.Lauritzen and R.Sah,IEEE Trans.Nucl.Sci.Vol. NS-28 No.3 June 1981
14. Geotechnical Investigations of the PEP site, R.S.Gould SLAC Internal Report PEP-206 February 1976

15. Geotechnical Investigation, Proposed Positron-Electron Project, Stanford Linear Accelerator Center, Stanford California, Dames and Moore, San Francisco. Job No.0651-130 June 1, 1977
16. Contract Drawings for the construction of the SLC North and South Arc tunnels, Tudor Engineering, San Francisco (ID 372-030-01 through ID372-030-10 )
17. Dynamic Isolation Systems, Inc. 2855 Telegraph Ave. Suite 410 Berkeley CA 94705, (415) 843-7233
18. "SLAC Site Geology, Ground Motion and Some Effects of the October 17th, 1989 Earthquake", G.E.Fischer, Report SLAC-358 December 1989.

**END**

**DATE FILMED**

11 / 15 / 90